Age and geochemistry of the Boucaut Volcanics in the Neoproterozoic Adelaide Rift Complex, South Australia

Sheree E Armistead*[1,2,3], Alan S Collins[1], Solomon Buckman[4] and Rachel Atkins[1]

[1]Tectonics and Earth Systems (TES) Group and the Mineral Exploration CRC, Department of Earth Sciences, The University of Adelaide, SA 5005, Australia

[2]Geological Survey of Canada, 601 Booth Street, Ottawa, Ontario, Canada

[3]Metal Earth, Harquail School of Earth Sciences, Laurentian University, Sudbury, Ontario, Canada

[4]School of Earth, Atmospheric and Life Sciences, University of Wollongong, Wollongong Australia

*corresponding author email: sarmistead@laurentian.ca

Keywords: Adelaide Rift Complex, Flinders Ranges, Geochemistry, Geochronology, Neoproterozoic, Rodinia, Snowball Earth, Adelaide Superbasin

ABSTRACT

The Adelaide Rift Complex in South Australia records the break-up of Rodinia at a time of great climatic and biological evolution. The Boucaut Volcanics within the Neoproterozoic Adelaide Rift Complex of the Adelaide Superbasin lie at the base of the Burra Group, marking the boundary between the Burra Group and underlying Callanna Group. Despite their significance as one of the few volcanic units within the rift complex, there has been no robust age determination published for the Boucaut Volcanics. We use U–Pb zircon LA-ICP-MS data to determine an age of 788 ± 6 Ma for the eruption of the bimodal Boucaut Volcanics. This has important implications for constraining the timing of stratigraphy within the Adelaide Superbasin. This also has far reaching implications for plate tectonic reconstructions of Australia and Laurentia, and for correlating global isotope anomalies for the Neoproterozoic.

1 INTRODUCTION

The Adelaide Superbasin in South Australia preserves Tonian to Middle Cambrian sedimentary and minor volcanic rocks (Lloyd et al., 2020; Preiss, 2000). They preserve some of the best evidence for the evolving, and sometimes tumultuous, events that characterise this time in Earth's climatic, biological and geological systems. For example, the earliest known complex multicellular lifeforms are preserved within the Ediacara Hills of the Flinders Ranges, and extensive tillites provide evidence for Earth's global Cryogenian glaciation events (Hoffman et al., 2017; Le Heron, Cox, Trundley, & Collins, 2011). Of significance to paleogeographic reconstructions, the Adelaide Rift Complex also contains rocks that have been interpreted as forming during the breakup of supercontinent Rodinia (Merdith, Collins, et al., 2017; Powell, Preiss, Gatehouse, Krapez, & Li, 1994; Preiss, 2000) (Figure 1). Understanding the tectonic and geological evolution of the Adelaide Rift Complex underpins our understanding of these significant Neoproterozoic events, not only in Australia, but globally.

One of the major challenges in reconstructing the evolution of the Adelaide Superbasin, is the lack of datable volcanic units and/or fossil assemblages that can provide quantitative age constraints on rifting and sedimentation. These challenges limit our ability to confidently correlate sequences in the Adelaide Superbasin with those in other regions.

1.1 Tectonic overview

The Neoproterozoic to middle Cambrian stratigraphy within the Adelaide Rift Complex formed during at least five major successive rift cycles that led to the breakup of supercontinent Rodinia (Preiss, 2000). In the Adelaide Rift Complex, initiation of the breakup of Rodinia is marked by the 827 ± 6 Ma Gairdner Dyke Swarm (Wingate, Campbell, Compston, & Gibson, 1998), which is interpreted to be coeval with the poorly dated Wooltana Volcanics (Compston, Crawford, & Bofinger, 1966). The second phase of rifting in the Adelaide Rift Complex is marked by the 802 ± 10 Ma Rook Tuff within the Callanna Group (pers. comm. Fanning 1994 in Preiss 2000). The third phase of rifting is marked by the Boucaut Volcanics. This rift phase marks the beginning of extensive syn-rift facies within the Adelaide Superbasin, yet, it has resisted attempts at dating and forms the focus of this study.

According to both the SWEAT (south-west US - East Antarctica; Dalziel, 1991; Moores, 1991) and AUSWUS (Australia-Western US; Burrett and Berry, 2000) hypotheses, the Laurentian and East Antarctic-Australian cratons were contiguous during the late Neoproterozoic. This has led to attempted correlations between the stratigraphy of the Adelaide Superbasin and western Laurentia. The SWEAT hypothesis posits a close link between southern Australia and NW

Canada. In this configuration the Boucaut Volcanics have been linked with the Little Dal Group of the Mackenzie Mountains in the Yukon-Northwest Territories of Canada (Milton, Hickey, Gleeson, & Friedman, 2017) (Figure 1 SWEAT reconstruction). Alternatively, the AUSWUS fit (Figure 1), the Adelaide Superbasin lies adjacent to south-western US, and correlations with stratigraphy in the Death Valley have been proposed (e.g. Dehler et al., 2017; Mahon et al., 2014). An analysis of kinematic data for the different reconstructions in Figure 1 showed that models that put Australia adjacent to southern Laurentia (e.g. AUSWUS, and a more extreme version with Australia adjacent to Mexico - AUSMEX, Wingate et al. 2002) are the easiest to reconcile with Phanerozoic plate kinematic norms (Merdith, Williams, Müller, & Collins, 2017).

On a smaller scale, correlations between the Adelaide Superbasin and northwest Tasmania have also been proposed, for example, between the c. 790 Ma Black River Dolomite of northwest Tasmania (Calver, 1998) and the Skillogallee Formation of the Adelaide Superbasin. However, more recent detrital provenance studies suggest that Neoproterozoic stratigraphy in Tasmania differs from the Adelaide Superbasin and instead correlate with rocks in the Death Valley in California and the Transantarctic Mountains (Mulder, Berry, Halpin, Meffre, & Everard, 2018).

Constraining correlations has important implications for paleogeographic reconstructions of Laurentia-Australia in the Rodinia supercontinent. Unfortunately, many of these correlations rely on old and/or unreliable age data, particularly for the Adelaide Superbasin (Figure 2).

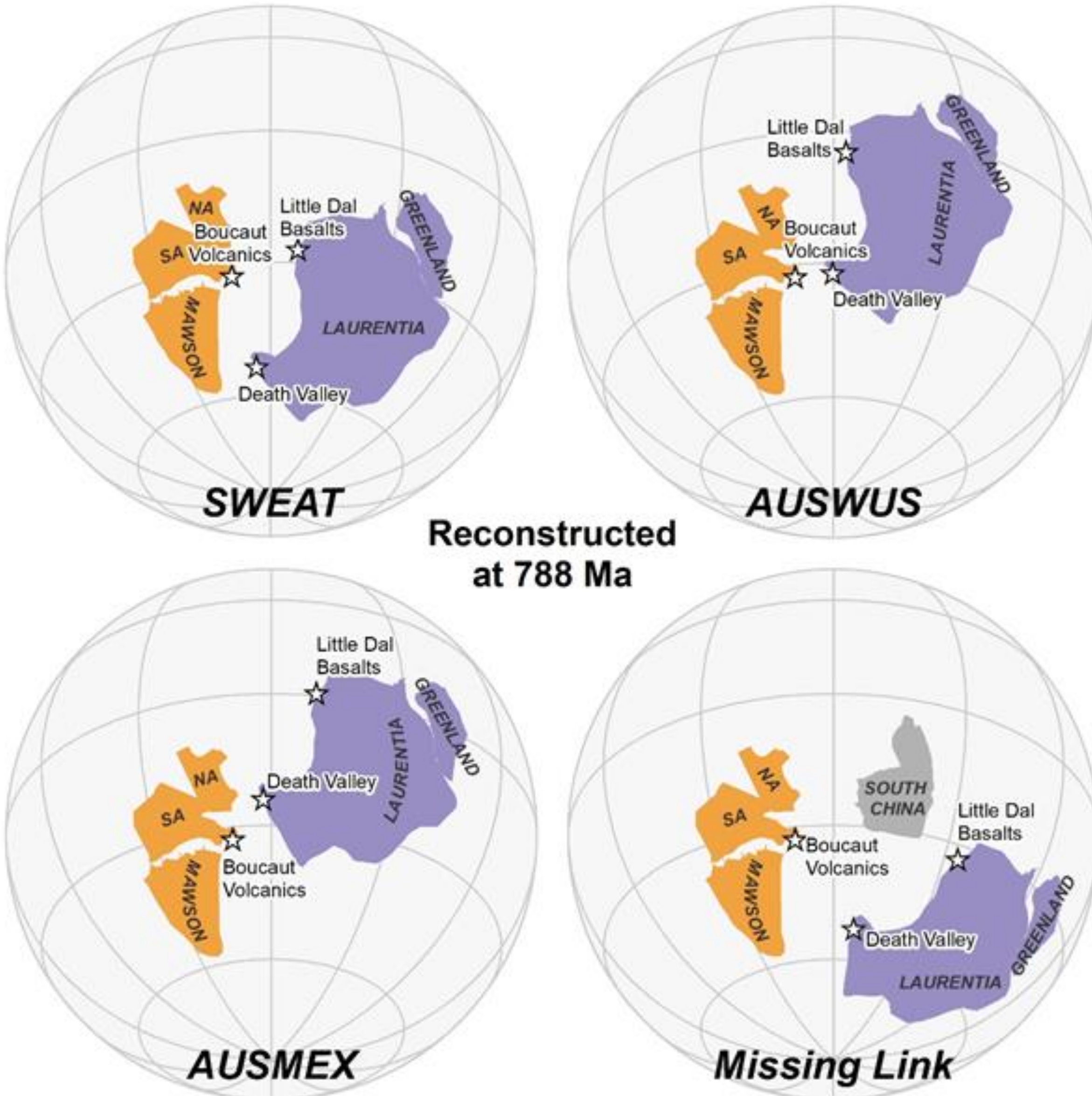

Figure 1: GPlates tectonic reconstructions of the different Australia-Laurentia models at 788 Ma (the crystallisation age of the Boucaut Volcanics), made using the models in Merdith, Williams, et al. (2017). South Australia is fixed in its present-day position with all other blocks rotated relative to it at 788 Ma. SWEAT reconstruction based on Dalziel (1991); Hoffman (1991); Moores (1991). AUSWUS reconstruction based on Karlstrom et al. (1999). AUSMEX reconstruction based on Wingate et al. (2002). Missing Link reconstruction based on Li, Zhang, and Powell (1995). NA = North Australia, SA = South Australia.

1.2 THE BOUCAUT VOLCANICS

The Boucaut Volcanics lie at the base of the Burra Group and provide an important maximum age constraint for this package. They also constrain the maximum age for the underlying Callanna Group. The age of the Boucaut Volcanics has been most widely reported as 777 ± 7 Ma (pers. comm. Fanning 1994 in Preiss 2000), however, no isotopic data are published for this associated age. Confusingly, another source (Drexel, Preiss, & Parker, 1993) mentions that Fanning (1989) derived an upper intercept age of 783 ± 42 Ma for the Boucaut Volcanics, but the original source of these data are obscure. Regardless, robust isotopic age determinations are needed to constrain the age of this significant unit.

The Boucaut Volcanics are dominated by pale pink to grey rhyolite, with amygdaloidal andesite and basalt also present (Forbes, 1978). These rocks have undergone several phases of deformation and have been metamorphosed to 'biotite grade' (Forbes, 1978). The Boucaut Volcanics occur within the southeastern part of the Nackara Arc, and the majority of outcrops are isolated and many are sheared along the northeast-trending Anabama Shear Zone (Preiss, 2000). The Boucaut Volcanics mark a major stage of rifting in the Adelaide Rift Complex that has been interpreted by many as reflecting the separation of Laurentia from Australia and the initiation of the Pacific Ocean basin (Preiss, 2000).

In this contribution, we have collected new U–Pb zircon data from a rhyolite within the Boucaut Volcanics, to provide a robust age constraint on the timing of eruption. Significantly, this new age constrains the base of the Burra Group and the onset of early rifting within the Adelaide Rift Complex, providing important constraints on plate reconstructions for the breakup of supercontinent Rodinia (e.g. Merdith et al., 2017a; Merdith et al., 2017b).

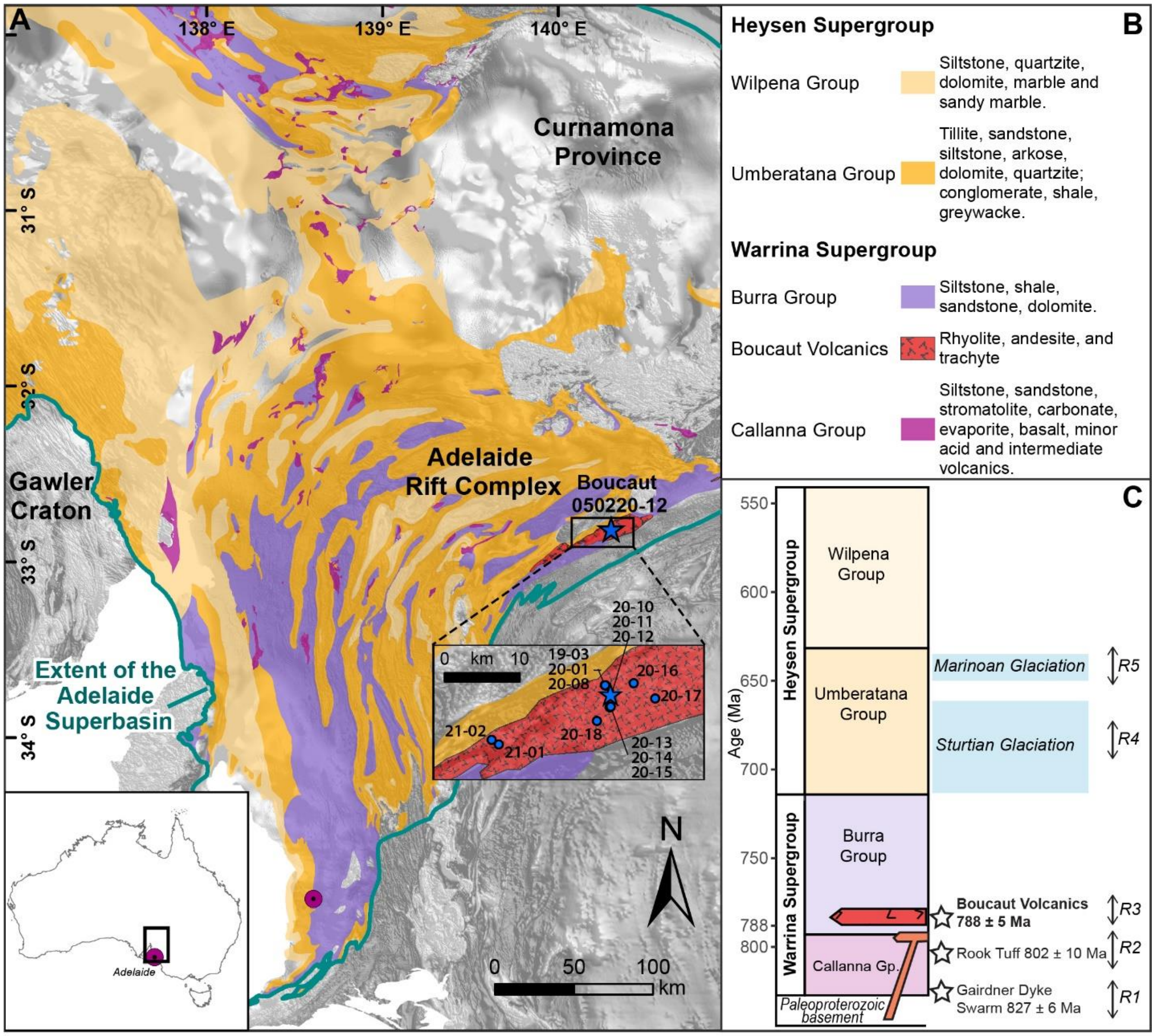

Figure 2: a) Geological map of the Adelaide Superbasin, including the Adelaide Rift Complex, overlying a total magnetic intensity, reduced to the pole image (source: SARIG). Location of geochronology sample indicated by the star (050220-12), whole-rock geochemistry samples indicated by circles in the inset (abbreviated; all samples have prefix 0502-). Extent of the Adelaide Superbasin after Lloyd et al. (2020). Geological polygons from SARIG. Coordinate system: GDA 1994; b) legend for geological map, descriptions for each unit from Australian Stratigraphic Units Database; and c) simplified tectono-stratigraphic history of the Adelaide Superbasin. R1–R5 mark the five major rifting events of the Adelaide Rift Complex. Rook Tuff date from Fanning, Ludwig, Forbes, and Preiss (1986), and Gairdner Dyke Swarm from Wingate et al. (1998).

2 ANALYTICAL METHODS

2.1 Zircon U–Pb and trace element geochemistry

A rhyolite sample from the Boucaut Volcanics (Sample 050220-12) was crushed and separated for zircons. Zircons were hand-picked and mounted in epoxy resin, and then polished and carbon coated. To identify suitable domains for analysis, zircons were imaged using a Gatan cathodoluminescence (CL) detector attached to Quanta 600 MLA Scanning Electron Microscope. Zircon U–Pb isotopic and REE/trace element determination was undertaken at the University of Adelaide using an Agilent 7900x ICP-MS with an attached ASI Resolution excimer 193nm laser ablation system. A spot size of 29 µm and frequency of 5 Hz was used and isotopes ^{90}Zr, ^{201}Hg, ^{204}Pb, ^{206}Pb, ^{207}Pb, ^{208}Pb, ^{232}Th and ^{238}U were measured. Each analysis comprised a 20s background and 30s ablation. GEMOC GJ-1 zircon was used to correct for U–Pb fractionation (TIMS normalising ages ^{207}Pb/^{206}Pb = 607.7 ± 4.3 Ma, ^{206}Pb/^{238}U = 600.7 ± 1.1 Ma and ^{207}Pb/^{235}U = 602.0 ± 1.0 Ma; Jackson et al. 2004). The Plešovice zircon standard was used to assess accuracy over the course of the laser session (ID TIMS ^{206}Pb/^{238}U = 337.13 ± 0.37 Ma; Sláma et al., 2008). Ten Plešovice standard analyses were made and yielded a weighted average ^{206}Pb/^{238}U age of 335.2 ± 4.1 Ma (2σ; MSWD=0.76), which is within uncertainty of the ID TIMS age. Data were processed using Iolite (Paton, Hellstrom, Paul, Woodhead, & Hergt, 2011). U–Pb data and REE data are provided in Supplementary A.

2.2 Whole-rock Geochemistry

Twenty-one samples from the Boucaut Volcanics were analysed for whole-rock geochemistry (see Figure 2a inset for sample locations). Major element geochemistry was obtained through the analysis of fused glass discs using X-Ray Fluorescence (XRF) at the University of Adelaide.

Trace and rare earth element geochemistry were undertaken by Amdel in Adelaide using IC3M and ICM3R. A subsample of up to 0.5 g of the analytical pulp was digested using an HF/multi acid digest and the solution was presented to an ICPMS for the quantification of the elements of interest. Geochemistry data are provided in Supplementary A.

3 RESULTS

3.1 Sample descriptions

The Boucaut Volcanics crop out near Boucaut East Dam, about 79 km south of Olary (Figure 2). Small isolated outcrops of highly vesicular basalt and rhyolite (Figure 3) are interbedded with thin beds of mudstone and some cross-bedded sandstones indicating a shallow marine environment during deposition of the basal Burra Group. Strain partitioning has resulted in preservation of undeformed pods of volcanics enveloped by strongly foliated equivalents. Minor copper mineralisation is associated with the basalts at Cronje Dam. The rhyolites sampled for this study were relatively fresh, fine-grained, flow-banded rhyolites with small (< 1 cm) phenocrysts of quartz and feldspar.

Sample descriptions and locations are provided in Table 1 and shown in Figure 2. Basalts were collected from the type section whilst rhyolites were collected from surrounding outcrops on the tops of small hills. Examples of outcrop textures are shown in Figure 3.

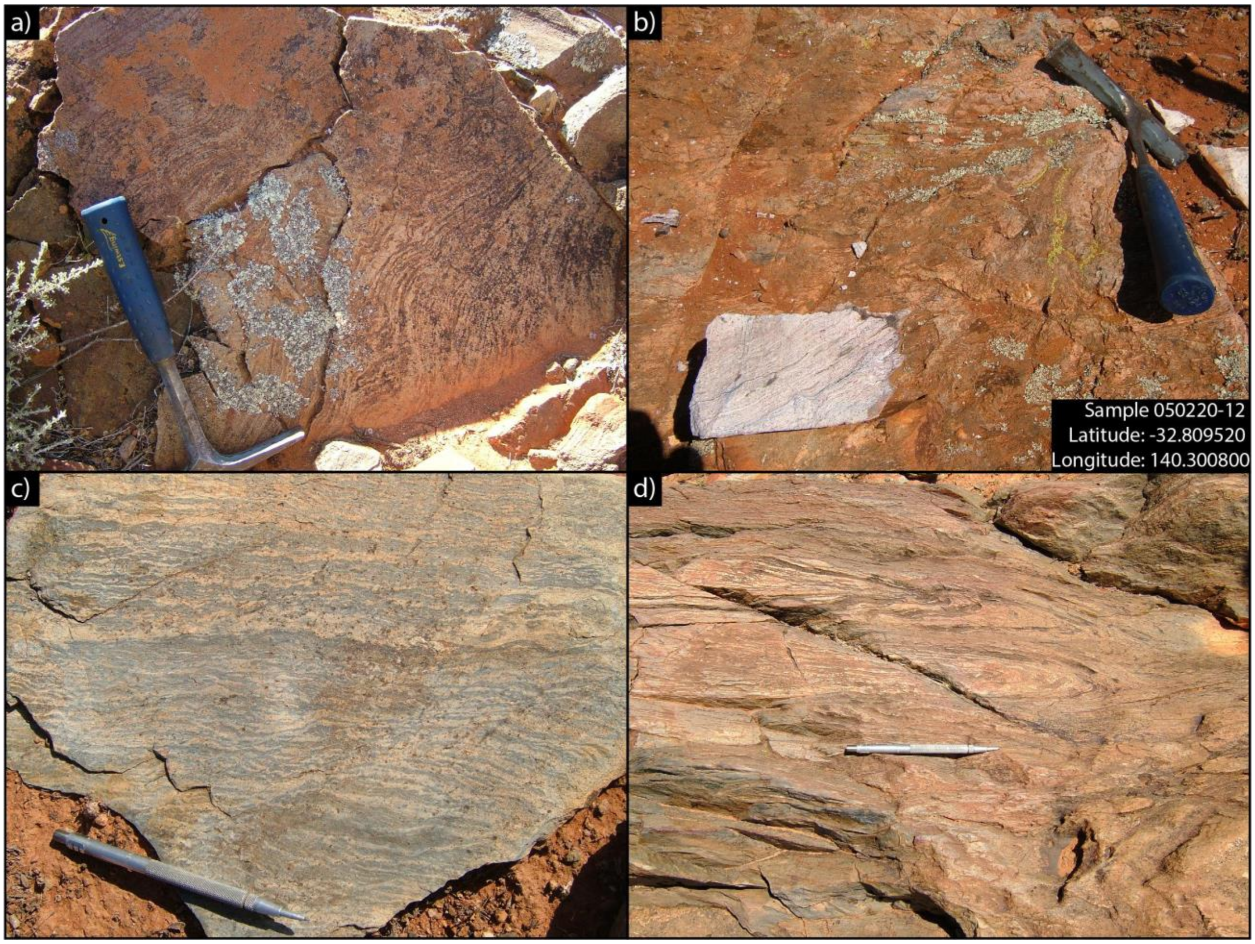

Figure 3: Field examples of the Boucaut Volcanics. a) flow banded rhyolite; b) Flow banded rhyolite. Fresh undeformed pod surrounded by foliated equivalent (Sample 050220-12); c) banded intermediate volcanic; d) flow banded or folded volcanic

Table 1: Sample descriptions, locations and analytical methods applied in this study.

Sample	Description	Analytical methods	Latitude	Longitude
050219-01	Anabama Mine. Metabasalt chips from RC drilling collar. Strong foliation, silicified, sericite	WR	-	-
050219-03	Boucaut volcanics type section. Fresh basalt with vesicles filled with epidote	WR	-32.799685	140.295644
050220-01	Boucaut volcanics type section	WR	-32.799685	140.295644
050220-02	Boucaut volcanics type section	WR	-32.799685	140.295644
050220-03	Boucaut volcanics type section	WR	-32.799685	140.295644
050220-04	Boucaut volcanics type section	WR	-32.799685	140.295644
050220-05	Boucaut volcanics type section	WR	-32.799685	140.295644

050220-06	Boucaut volcanics type section	WR	-32.799685	140.295644
050220-07	Boucaut volcanics type section	WR	-32.799685	140.295644
050220-08	Boucaut volcanics type section	WR	-32.799685	140.295644
050220-10	Boucaut felsic volcanic	WR	-32.808832	140.300485
050220-11	Boucaut felsic volcanic - foliated 309/73	WR	-32.808832	140.300485
050220-12	Boucaut felsic volcanic. Fresh undeformed pod surrounded by foliated equivalent	WR + geochronology	-32.809520	140.300800
050220-13	Boucaut felsic volcanic - tuff?	WR	-32.825849	140.301249
050220-14	Rhyolite with flow banding bedding 179/75	WR	-32.825895	140.301409
050220-15	Rhyolite with flow banding bedding	WR	-32.825258	140.302055
050220-16	Rhyolite. Glassy K-spar rich	WR	-32.797221	140.329893
050220-17	Meta basalt chips from drillcore collar CRD15. Some chalcopyrite mineralisation	WR	-32.815613	140.355403
050220-18	Rhyolite. Round clasts? K-spar rind, flow banding. Bedding 335/71	WR	-32.842648	140.285837
050221-01	Rhyolite with flow banding bedding. Foliation and crenulation in parts. Bedding 335/85	WR	-32.870726	140.168623
050221-02	Cronje Dam prospect Cu. Malachite along foliation	WR	-32.865131	140.160146

3.2 Zircon U–Pb geochronology and trace element geochemistry

Separated zircons from sample 050220-12 are generally euhedral with preserved facets and pyramidal terminations. Most zircons are either banded or have concentric oscillatory zoning in CL images (Figure 4). Forty-four U–Pb and trace element analyses were obtained from 41 zircons, of which 39 are within 10% of concordance and 29 are within 5% of concordance (Figure 5). The 29 analyses within 5% concordance yield a $^{206}Pb/^{238}U$ weighted average age of 788 ± 6 Ma (MSWD = 1.08), which we interpret as the crystallisation age of this sample. A $^{207}Pb/^{206}Pb$ weighted average of the same analyses yielded an age of 786 ± 13 Ma (MSWD = 0.29).

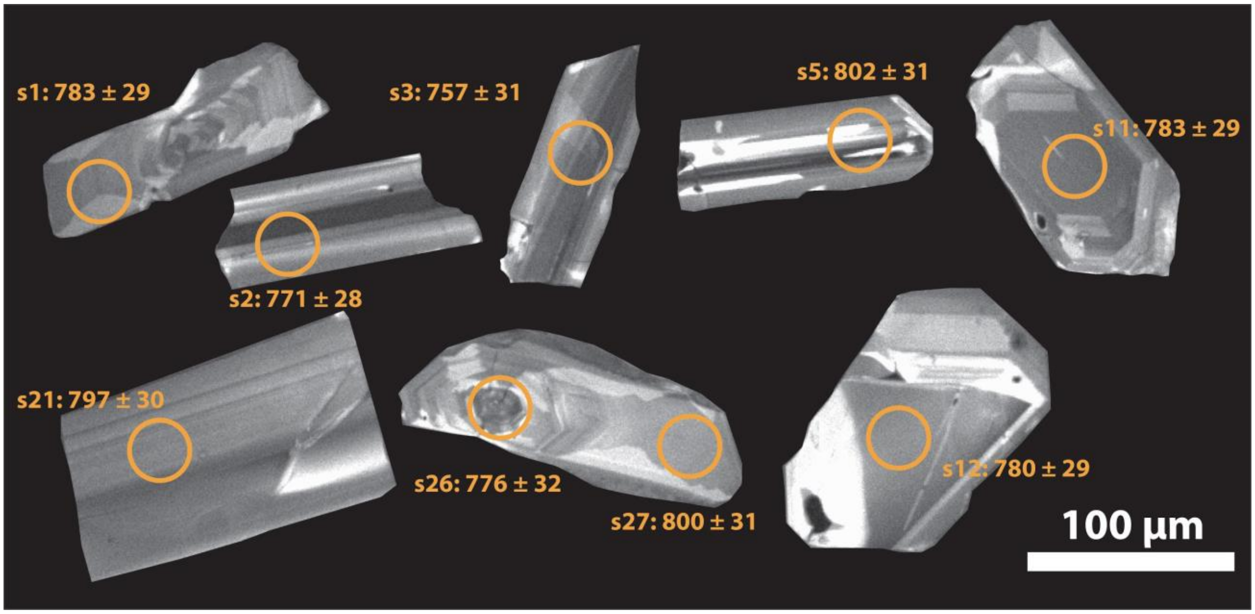

Figure 4: Examples of CL images for analysed zircons.

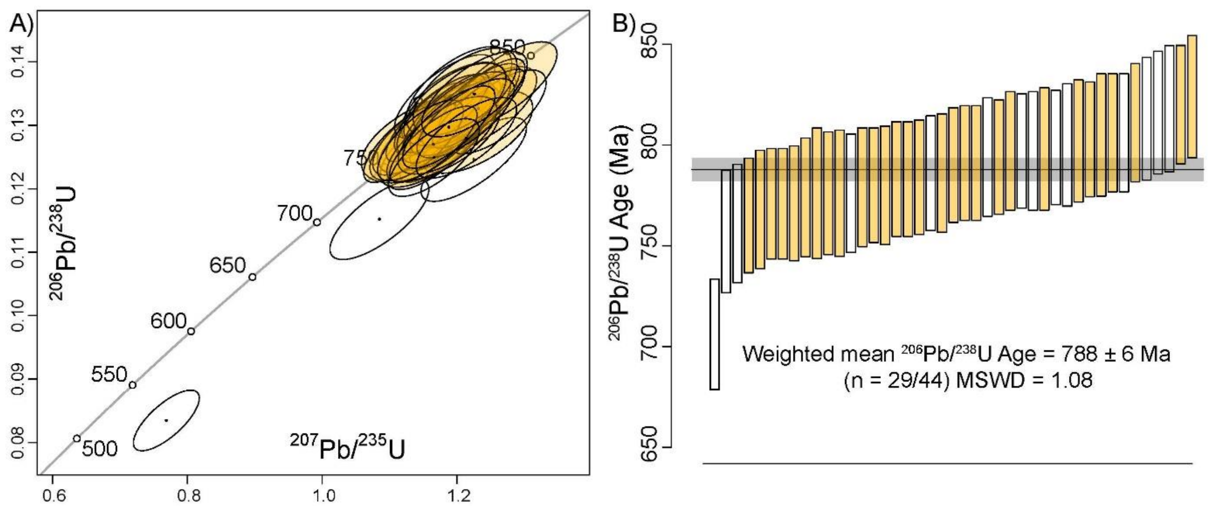

Figure 5: a) Conordia plot of U–Pb data, data within 5% of concordance are included in age calculations (orange ellipses), and excluded data are interpreted as Pb-loss (white ellipses); b) Weighted average plot of the same data shown in (a). Plots and data produced using IsoplotR (Vermeesch, 2018).

Trace element profiles from analyses that are within 10% of concordance are shown in Figure 6 along with their Th/U ratios. Zircons show Th/U values between 0.5 and 1.2 that are consistent with igneous zircons (Belousova, Griffin, O'Reilly, & Fisher, 2002). The majority of near concordant zircon divide into two coupled Th/U and REE populations (Figure 6). One population has Th/U ratios >0.8, elevated rare earth elements and moderate positive Ce anomalies. The second population has Th/U ratios <0.8 and a pronounced positive Ce anomaly. Both populations have moderate negative Eu anomalies and positive medium to high rare earth element gradients. The negative Eu anomaly can be caused by the presence of plagioclase in the magma that the zircon grew in, and/or by a reducing magma. The latter possibility is discounted as a positive Ce anomaly is a sign of an oxidising magma (Trail, Watson, & Tailby, 2012). Additionally, Kirkland, Smithies, Taylor, Evans, and McDonald (2015) showed that Th/U ratios positively correlate with temperature in a cooling fractionating magma due to the preferential magma depletion of U as the magma cools. We use these observations to suggest that our analysed zircons reflect growth in a cooling fractionating magma chamber that was becoming progressively more oxidized as it cooled.

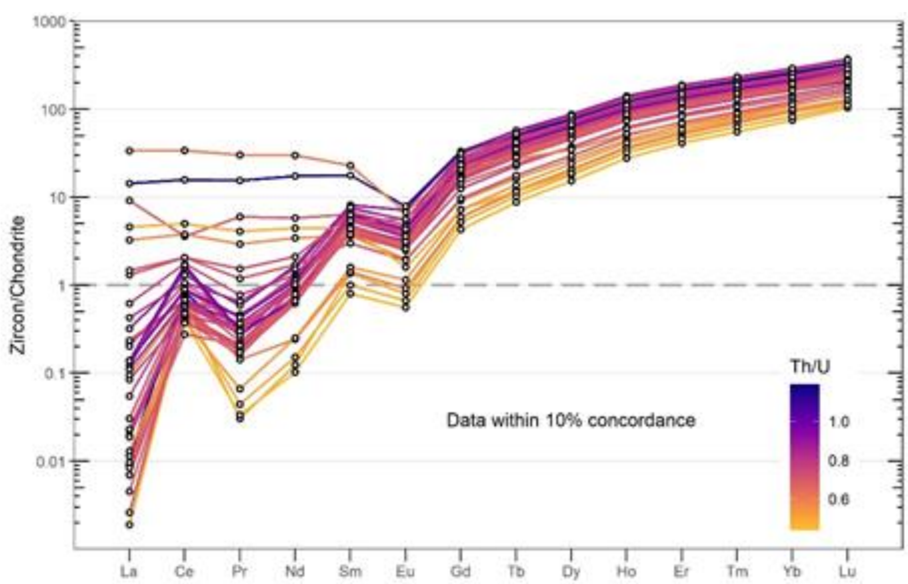

Figure 6: Trace element profile of zircons within 10% concordance (n=39/44), coloured by Th/U. Normalised to Chondrite (Sun & McDonough, 1989).

3.4 Whole-rock geochemistry

Rock samples from the Boucaut Volcanics range from basaltic to rhyolitic compositions, with SiO_2 ranging from 45% to 79% (Figure 7a). Around half of the samples plot within the rhyolite field on a total alkali silica (TAS) diagram (Le Bas, Le Maitre, Streckeisen, Zanettin, & Rocks, 1986), with the remaining samples plotting within the basalt, andesite and dacite fields. Samples range from ferroan to magnesian.

On the REE diagram of sample/chondrite (Figure 7c), samples are enriched in LREE over HREE, with some exhibiting a negative Eu anomaly indicating plagioclase fractionation.

On the sample/primitive mantle REE diagram, samples show a strong negative Sr anomaly, which is more pronounced for the felsic samples. Samples show a strong positive Pb anomaly, with this signature being more pronounced for mafic samples.

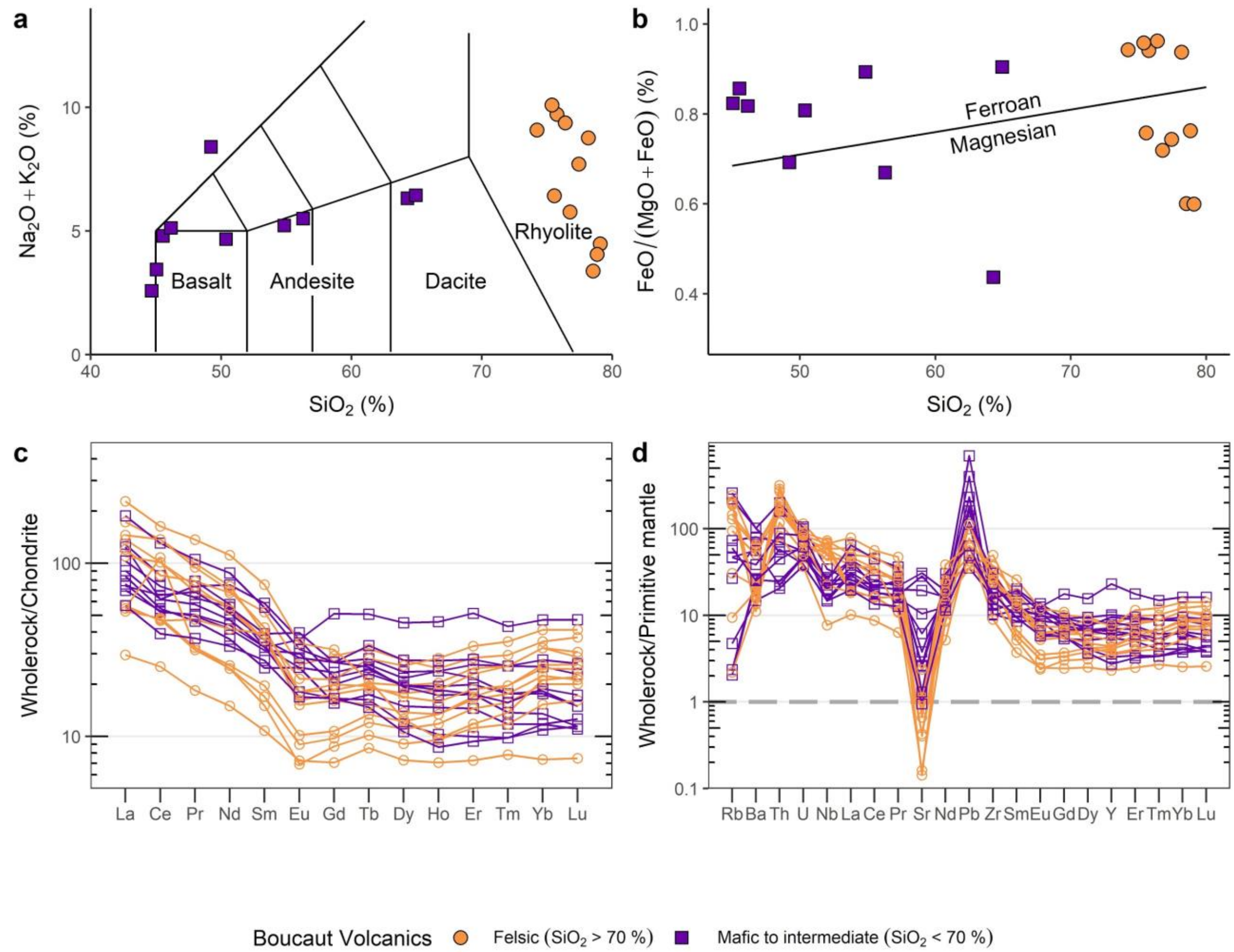

Figure 7: Whole-rock geochemistry plots a) total Alkali vs. Silica plot after Le Bas et al., 1986; b) Ferroan/Magnesian vs. Silica plot after Frost and Frost 2008; c) REE normalised to Chondrite (Sun & McDonough, 1989); d) Trace elements normalised to primitive mantle.

4 DISCUSSION AND IMPLICATIONS

Here we present a revised age for the eruption of the Boucaut Volcanics at 788 ± 6 Ma along with whole-rock geochemistry for a range of samples from the Boucaut Volcanics. This age is older than a poorly documented age of 777 ± 7 Ma that was based on a personal communication with no associated isotopic data. The new age presented here provides important constraints on early rifting in the Adelaide Rift Complex, and provides a piercing point for plate tectonic reconstructions. The revised age of 788 ± 6 Ma constrains the onset of the third phase of rifting in the Adelaide Rift Complex (Figure 2c) to be as early as 788 ± 6 Ma, earlier than previously suggested (Preiss, 2000), but more consistent with kinematic constraints on the timing of the Australia–Laurentia rift-drift transition as central Rodina broke up (Merdith et al. 2017b).

This new age of the Boucaut Volcanics constrains the base of the Burra Group to 788 ± 6 Ma. The underlying Callanna Group, has a reported maximum age of 802 ± 10 Ma (Fanning et al., 1986), which, however, is only documented in an abstract with no isotopic data. The Callanna Group appears not to contain the ca. 810 Ma Bitter Springs carbon isotope anomaly (Macdonald et al. 2010; Stueken et al. 2019), which may be used as a minimum age constraint. Although more work needs to confirm that the basin waters had compositions similar to the contemporaneous ocean waters. Our new data now provide a revised minimum age for the deposition of the Callanna Group of 788 ± 6 Ma.

Several intrusive and extrusive magmatic suites are present within the Adelaide Superbasin. Due to the scarcity of robust age constraints, these have been challenging to place within a tectonostratigraphic framework, and to correlate with other units across the region. The Kooringa Member within the Skillogallee Dolomite contains an intrusive porphyry that has been data at 794 ± 4 Ma (Preiss et al., 2009). This is within uncertainty of the Boucaut Volcanics and may represent an intrusive equivalent.

ACKNOWLEDGEMENTS

Jarred Lloyd and Claire Wade are thanked for providing regional overview data and context. ASC acknowledged the MinEx CRC and his contribution forms MinEx CRC output #2020/xx. Sarah Gilbert and Ben Wade at Adelaide Microscopy are thanked for help obtaining analytical data.

REFERENCES

Belousova, E., Griffin, W. L., O'Reilly, S. Y., & Fisher, N. (2002). Igneous zircon: trace element composition as an indicator of source rock type. *Contributions to mineralogy and petrology, 143*(5), 602-622.

Burrett, C., & Berry, R. (2000). Proterozoic Australia–Western United States (AUSWUS) fit between Laurentia and Australia. *Geology, 28*(2), 103-106.

Calver, C. (1998). Isotope stratigraphy of the Neoproterozoic Togari Group, Tasmania. *Australian Journal of Earth Sciences, 45*(6), 865-874.

Compston, W., Crawford, A., & Bofinger, V. (1966). A radiometric estimate of the duration of sedimentation in the Adelaide Geosyncline, South Australia. *Journal of the Geological Society of Australia, 13*(1), 229-276.

Dalziel, I. W. (1991). Pacific margins of Laurentia and East Antarctica-Australia as a conjugate rift pair: Evidence and implications for an Eocambrian supercontinent. *Geology, 19*(6), 598-601.

Dehler, C., Gehrels, G., Porter, S., Heizler, M., Karlstrom, K., Cox, G., . . . Timmons, M. (2017). Synthesis of the 780–740 Ma Chuar, Uinta Mountain, and Pahrump (ChUMP) groups, western USA: implications for Laurentia-wide cratonic marine basins. *Bulletin, 129*(5-6), 607-624.

Drexel, J., Preiss, W., & Parker, A. (1993). The geology of South Australia, vol. 1. The Precambrian: South Australia Geological Survey. *Bulletin, 54*, 242.

Fanning, C. (1989). U-Pb dating of the Boucaut Volcanics and Bendigo Granite. *Amdel report G, 7948*.

Fanning, C., Ludwig, K., Forbes, B., & Preiss, W. (1986). *Single and multiple grain U–Pb zircon analyses for the early Adelaidean Rook Tuff, Willouran Ranges, South Australia.* Paper presented at the Geological Society of Australia Abstracts.

Forbes, B. G. (1978). The Boucaut Volcanics. *The Geological Survey of South Australia Quarterley Geological Notes*(65), 6–10.

Frost, B. R., & Frost, C. D. (2008). A geochemical classification for feldspathic igneous rocks. *Journal of petrology, 49*(11), 1955-1969.

Hoffman, P. F. (1991). Did the breakout of Laurentia turn Gondwanaland inside-out? *Science, 252*(5011), 1409-1412.

Hoffman, P. F., Abbot, D. S., Ashkenazy, Y., Benn, D. I., Brocks, J. J., Cohen, P. A., . . . Erwin, D. H. (2017). Snowball Earth climate dynamics and Cryogenian geology-geobiology. *Science Advances, 3*(11), e1600983.

Jackson, S. E., Pearson, N. J., Griffin, W. L., & Belousova, E. A. (2004). The application of laser ablation-inductively coupled plasma-mass spectrometry to in situ U–Pb zircon geochronology. *Chemical Geology, 211*(1), 47-69.

Karlstrom, K. E., Harlan, S. S., Williams, M. L., McLelland, J., Geissman, J. W., & Ahall, K.-I. (1999). Refining Rodinia: Geologic evidence for the Australia–western US connection in the Proterozoic. *GSA Today, 9*(10), 1-7.

Kirkland, C., Smithies, R., Taylor, R., Evans, N., & McDonald, B. (2015). Zircon Th/U ratios in magmatic environs. *Lithos, 212*, 397-414.

Le Bas, M., Le Maitre, R., Streckeisen, A., Zanettin, B., & Rocks, I. S. o. t. S. o. I. (1986). A chemical classification of volcanic rocks based on the total alkali-silica diagram. *Journal of petrology, 27*(3), 745-750.

Le Heron, D. P., Cox, G., Trundley, A., & Collins, A. S. (2011). Two Cryogenian glacial successions compared: Aspects of the Sturt and Elatina sediment records of South Australia. *Precambrian Research, 186*(1-4), 147-168.

Li, Z.-X., Zhang, L., & Powell, C. M. (1995). South China in Rodinia: part of the missing link between Australia–East Antarctica and Laurentia? *Geology, 23*(5), 407-410.

Lloyd, J. C., Blades, M. L., Counts, J. W., Collins, A. S., Amos, K. J., Wade, B. P., . . . Shahin, S. (2020). Neoproterozoic Geochronology and Provenance of the Adelaide Superbasin. *Precambrian Research*, 105849.

Mahon, R. C., Dehler, C. M., Link, P. K., Karlstrom, K. E., & Gehrels, G. E. (2014). Detrital zircon provenance and paleogeography of the Pahrump Group and overlying strata, Death Valley, California. *Precambrian Research, 251*, 102-117.

Merdith, A. S., Collins, A. S., Williams, S. E., Pisarevsky, S., Foden, J. D., Archibald, D. B., . . . Plavsa, D. (2017). A full-plate global reconstruction of the Neoproterozoic. *Gondwana Research, 50*, 84-134.

Merdith, A. S., Williams, S. E., Müller, R. D., & Collins, A. S. (2017). Kinematic constraints on the Rodinia to Gondwana transition. *Precambrian Research, 299*, 132-150.

Milton, J. E., Hickey, K. A., Gleeson, S. A., & Friedman, R. M. (2017). New U-Pb constraints on the age of the Little Dal Basalts and Gunbarrel-related volcanism in Rodinia. *Precambrian Research, 296*, 168-180.

Moores, E. (1991). Southwest US-East Antarctic (SWEAT) connection: a hypothesis. *Geology, 19*(5), 425-428.

Mulder, J. A., Berry, R. F., Halpin, J. A., Meffre, S., & Everard, J. L. (2018). Depositional age and correlation of the Oonah Formation: refining the timing of Neoproterozoic basin formation in Tasmania. *Australian Journal of Earth Sciences, 65*(3), 391-407. doi:10.1080/08120099.2018.1426629

Paton, C., Hellstrom, J., Paul, B., Woodhead, J., & Hergt, J. (2011). Iolite: Freeware for the visualisation and processing of mass spectrometric data. *Journal of Analytical Atomic Spectrometry, 26*(12), 2508-2518.

Powell, C. M., Preiss, W., Gatehouse, C., Krapez, B., & Li, Z.-X. (1994). South Australian record of a Rodinian epicontinental basin and its mid-Neoproterozoic breakup (~ 700 Ma) to form the Palaeo-Pacific Ocean. *Tectonophysics, 237*(3-4), 113-140.

Preiss, W. (2000). The Adelaide Geosyncline of South Australia and its significance in Neoproterozoic continental reconstruction. *Precambrian Research, 100*(1-3), 21-63.

Sláma, J., Košler, J., Condon, D. J., Crowley, J. L., Gerdes, A., Hanchar, J. M., . . . Norberg, N. (2008). Plešovice zircon—a new natural reference material for U–Pb and Hf isotopic microanalysis. *Chemical Geology, 249*(1), 1-35.

Sun, S.-S., & McDonough, W.-S. (1989). Chemical and isotopic systematics of oceanic basalts: implications for mantle composition and processes. *Geological Society, London, Special Publications, 42*(1), 313-345.

Trail, D., Watson, E. B., & Tailby, N. D. (2012). Ce and Eu anomalies in zircon as proxies for the oxidation state of magmas. *Geochimica et Cosmochimica Acta, 97*, 70-87.

Vermeesch, P. (2018). IsoplotR: A free and open toolbox for geochronology. *Geoscience Frontiers, 9*(5), 1479-1493.

Wingate, M. T., Campbell, I. H., Compston, W., & Gibson, G. M. (1998). Ion microprobe U–Pb ages for Neoproterozoic basaltic magmatism in south-central Australia and implications for the breakup of Rodinia. *Precambrian Research, 87*(3-4), 135-159.

Wingate, M. T., Pisarevsky, S. A., & Evans, D. A. (2002). Rodinia connections between Australia and Laurentia: no SWEAT, no AUSWUS? *Terra Nova, 14*(2), 121-128.